SAND2015-1951C

Materials challenges for a novel wind turbine rotary electrical contact technology

From the SNL Materials Science and Engineering Center in New Mexico:

Nicolas Argibay, Michael T. Dugger, Brad L. Boyce, Brendan L. Nation, Bradley Salzbrenner, Tomas F. Babuska

From the SNL Transportation Energy Center in California:

Jeffrey P. Koplow, Wayne L. Staats, Justin W. Vanness, Kent S. Smith, Arthur K. Harumichi

TMS2015
144th Annual Meeting & Exhibition

Sandia National Laboratories

National Nuclear Security Administration

U.S. DEPARTMENT OF ENERGY

Sandia National Laboratories is a multi-program laboratory managed and operated by Sandia Corporation, a wholly owned subsidiary of Lockheed Martin Corporation, for the U.S. Department of Energy's National Nuclear Security Administration under contract DE-AC04-94AL85000

How Economies-of-Scale is Shaping Technological Change in Wind Power

Economies of scale driving toward 10+ MW turbines

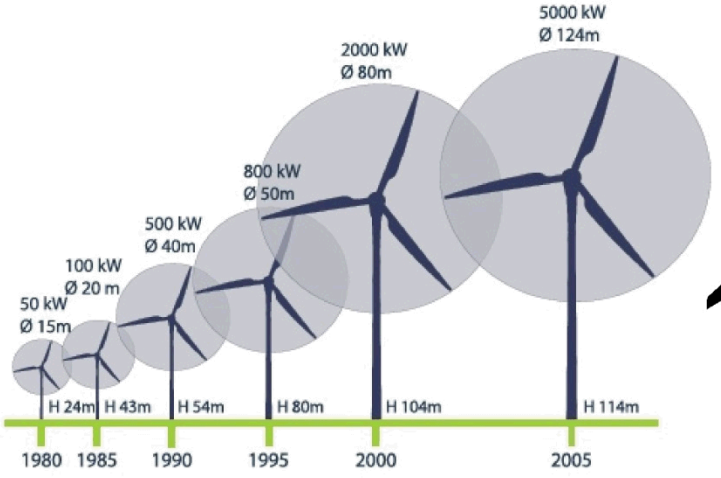

ref: http://www.terramagnetica.com/2009/08/01/why-are-wind-turbines-getting-bigger/

747 wingspan is 60m

ref: http://www.airvectors.net

price change was the difference between $25k or $1.25M in cost of Nd alone for 10 MW turbine, equivalent to < 1% to ~ 10% the cost of a turbine

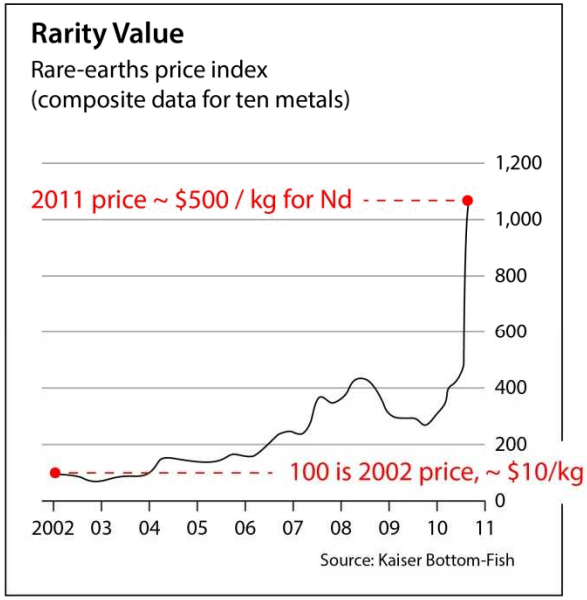

Key Technological Challenges:

1. Improve reliability -- direct drive (no gearboxes)
   Implies the use of high pole count synchronous generators, requiring about 250 kg/MW of Nd

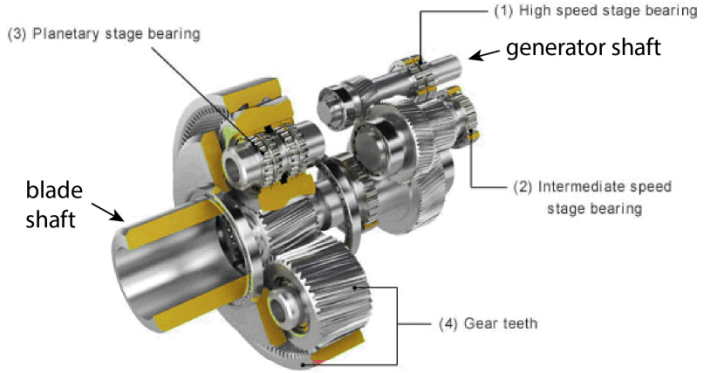

ref: http://www.olympus-ims.com/en/applications/rvi-wind-turbine/

2. Avoid rare earth metals -- a 2011 DOE Critical Materials Strategy report described the volatility of rare earth metals supply as the key challenge facing renewable energy technology development

ref: http://www.ars.usda.gov/is/graphics/photos/jun05/d115-1.htm (photo by Peggy Greb)

A Macro-Scale View: the Potential Impact and Role of Wind Power

Jacobson and Delucchi analyzed the feasibility and viability of achieving the goal of providing 100% of global energy needs via wind, water and solar energy harvesting by 2030 based on trends in technology development...

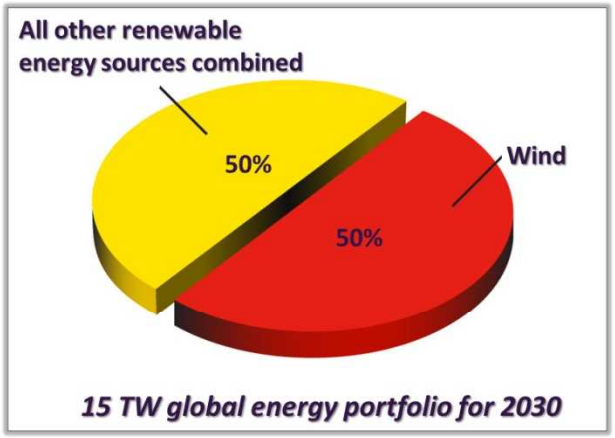

at $0.04 / kW-h (highly competitive even today)

Energy Policy 39 (2011) 1154–1169

Contents lists available at ScienceDirect

Energy Policy

journal homepage: www.elsevier.com/locate/enpol

Providing all global energy with wind, water, and solar power, Part I: Technologies, energy resources, quantities and areas of infrastructure, and materials

Mark Z. Jacobson [a,*], Mark A. Delucchi [b,1]

[a] Department of Civil and Environmental Engineering, Stanford University, Stanford, CA 94305-4020, USA
[b] Institute of Transportation Studies, University of California at Davis, Davis, CA 95616, USA

ARTICLE INFO

Article history:
Received 3 September 2010
Accepted 22 November 2010
Available online 30 December 2010

Keywords:
Wind power
Solar power
Water power

ABSTRACT

Climate change, pollution, and energy insecurity are among the greatest problems of our time. Addressing them requires major changes in our energy infrastructure. Here, we analyze the feasibility of providing worldwide energy for all purposes (electric power, transportation, heating/cooling, etc.) from wind, water, and sunlight (WWS). In Part I, we discuss WWS energy system characteristics, current and future energy demand, availability of WWS resources, numbers of WWS devices, and area and material requirements. In Part II, we address variability, economics, and policy of WWS energy. We estimate that ~3,800,000 5 MW wind turbines, ~49,000 300 MW concentrated solar plants, ~40,000 300 MW solar PV power plants, ~1.7 billion 3 kW rooftop PV systems, ~5350 100 MW geothermal power plants, ~270 new 1300 MW hydroelectric power plants, ~720,000 0.75 MW wave devices, and ~490,000 1 MW tidal turbines can power a 2030 WWS world that uses electricity and electrolytic hydrogen for all purposes. Such a WWS infrastructure reduces world power demand by 30% and requires only ~0.41% and ~0.59% more of the world's land for footprint and spacing, respectively. We suggest producing all new energy with WWS by 2030 and replacing the pre-existing energy by 2050. Barriers to the plan are primarily social and political, not technological or economic. The energy cost in a WWS world should be similar to that today.

Power available in energy resource worldwide if the energy is used in conversion devices, in locations where the energy resource is high, in likely-developable locations, and in delivered electricity in 2005 or 2007 (for wind and solar PV).

Energy technology	Power worldwide (TW)	Power in high-energy locations (TW)	Power in likely-developable locations (TW)	Current power delivered as electricity (TW)
Wind	1700[a]	72–170[b]	40–85[c]	0.02[d]
Wave	> 2.7[d]	2.7[e]	0.5[d]	0.000002[d]
Geothermal	45[f]	2[g]	0.07-0.14[d]	0.0065[d]
Hydroelectric	1.9[d]	< 1.9[d]	1.6[d]	0.32[d]
Tidal	3.7[d]	0.8[d]	0.02[d]	0.00006[d]
Solar PV	6500[h]	1300[i]	340[d]	0.0013[d]
CSP	4600[j]	920[j]	240[j]	000046[d]

Where the winds are: off-shore hydrogen production

Off-shore wind energy harvesting resolves the NIMBY (not in my back yard problem)...

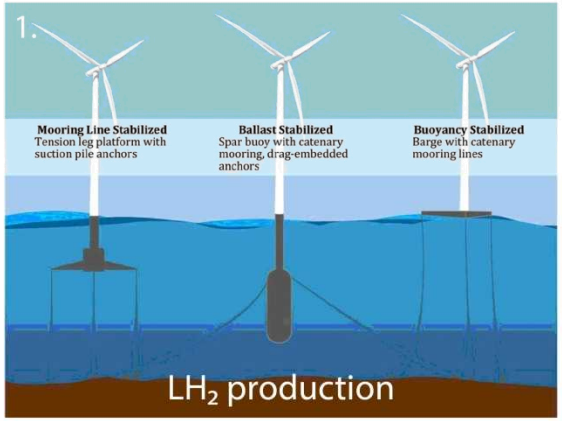

... as well as the diurnal averaging problem.

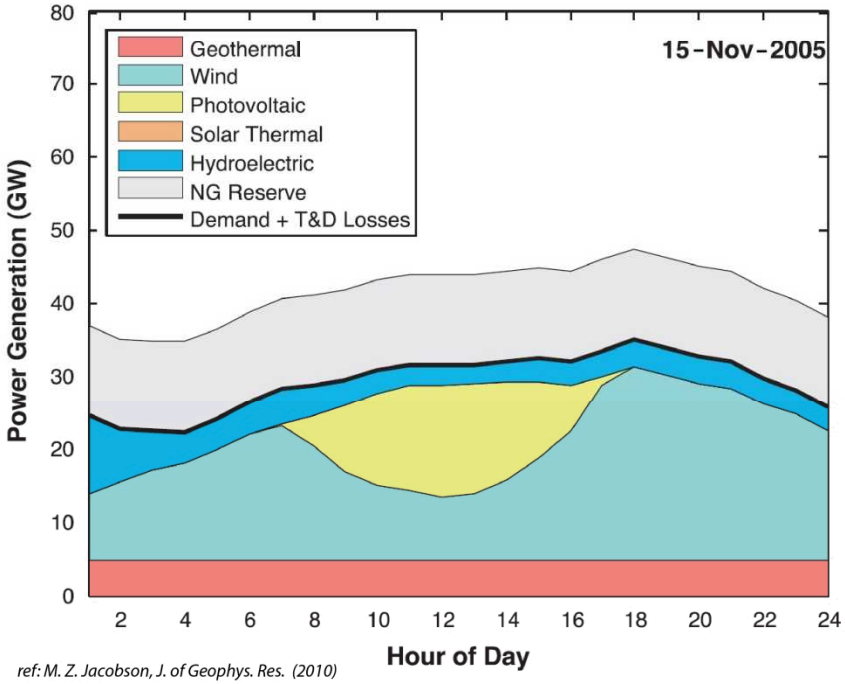

ref: M. Z. Jacobson, J. of Geophys. Res. (2010)

average wind speeds (m/s)

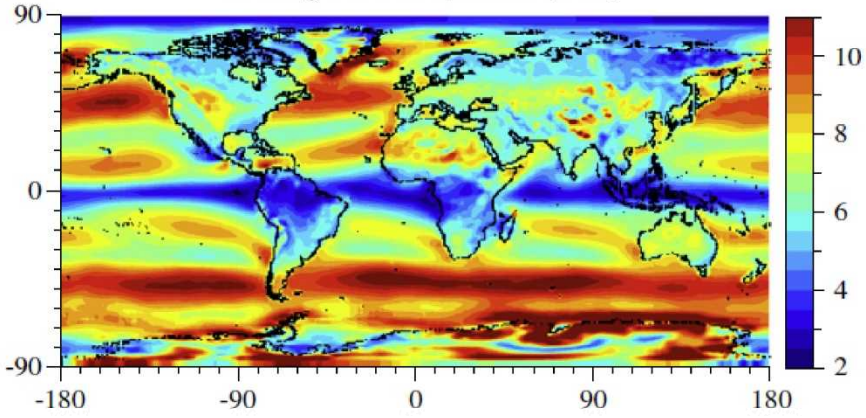

ref: M. Z. Jacobson, J. of Geophys. Res. (2010)

Standing technological challenges:

1. Rare earth magnets (REMs) are economically and environmentally problematic
2. Maintenance schedules of REM-free generators are impractical for off-shore use

Wire-Wound Direct-Drive Generators Necessitate an Electrical Contact

With Gearbox
(250 kg Nd/MW!)

No Gearbox (Direct-Drive)
(No REMs, wire wound rotor and stator magnets)

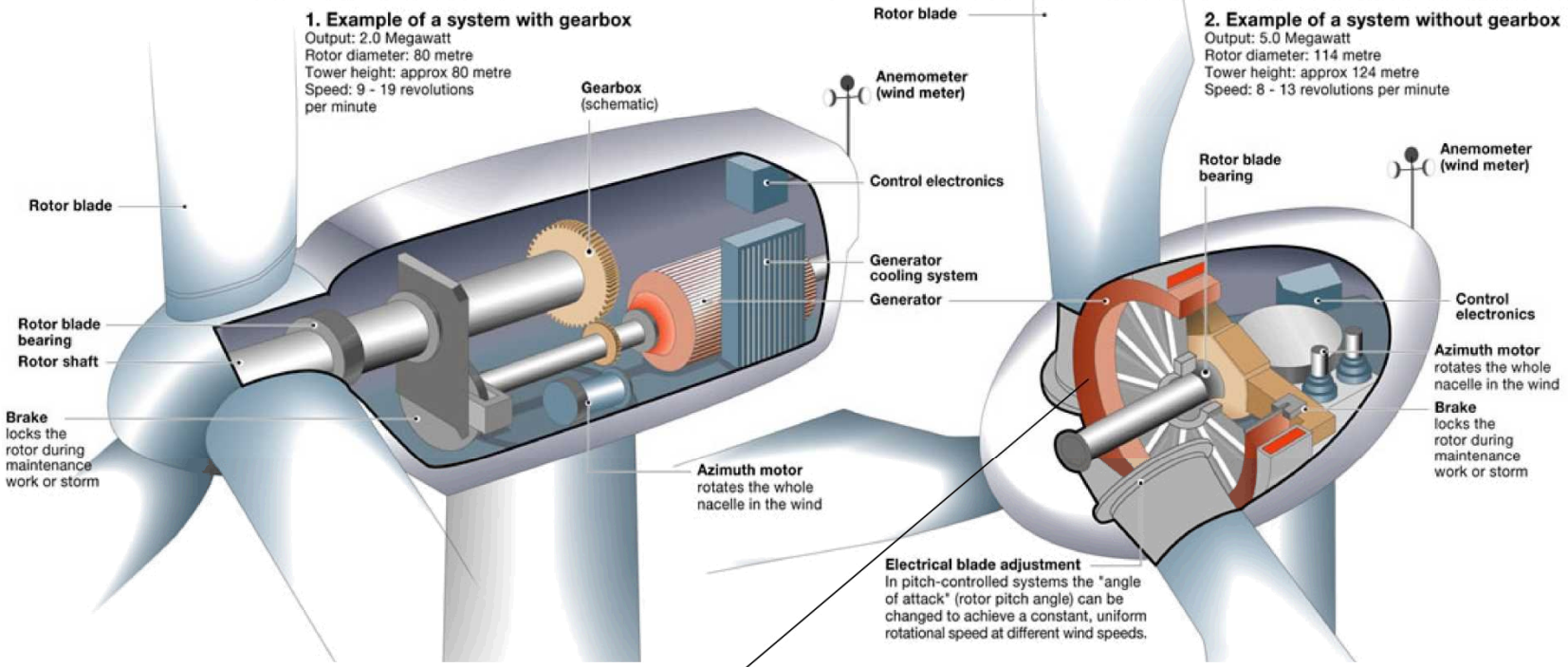

Courtesy of Enercon GmbH

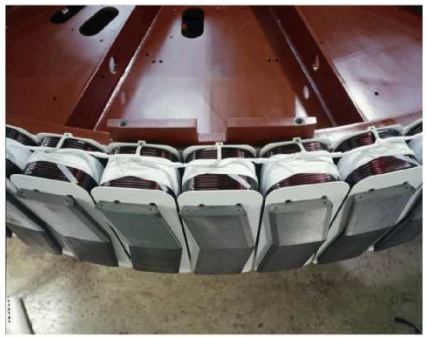

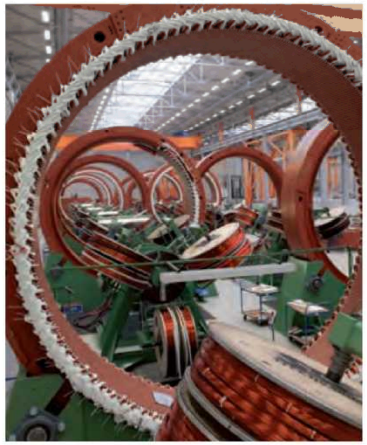

Wire-wound magnets to replace permanent magnets

→ Requires an electrical contact:

Sandia Labs "Twistact"

- 30 year life
- 100M rotations
- maintenance free
- low resistance (~ 1 mΩ)
- > 1kA capacity

Twistact Topology and Advanced Concepts

Rendering of 1-channel Twistact

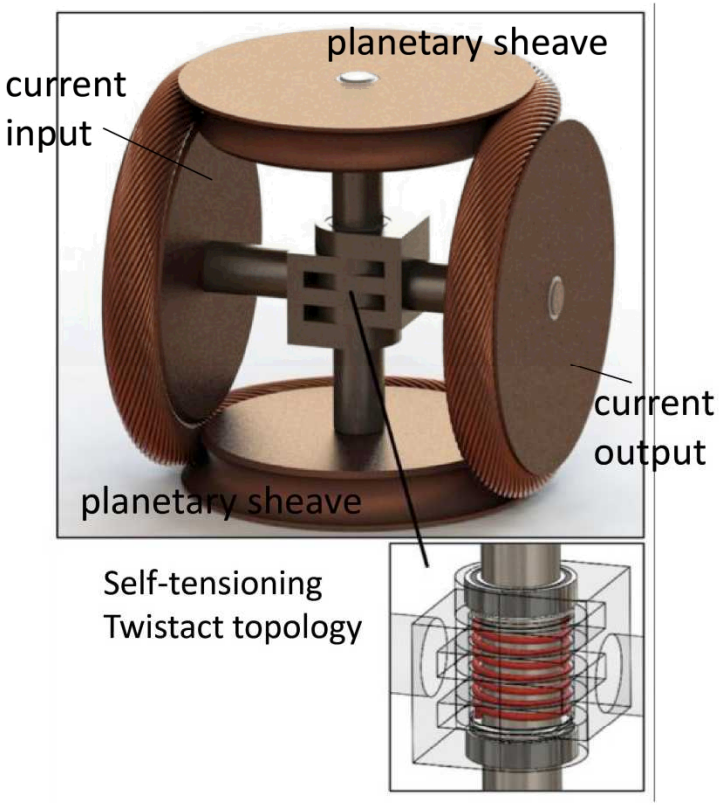

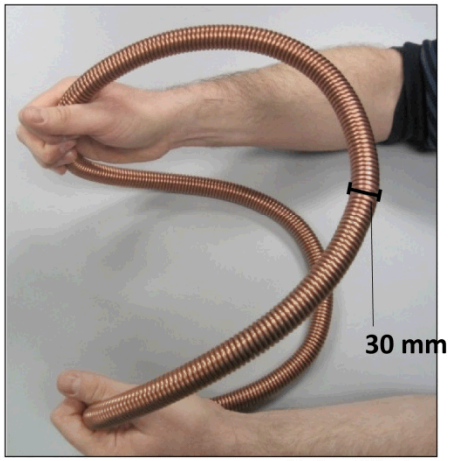

wire-wound endless Cu helical belt

2-channel DC

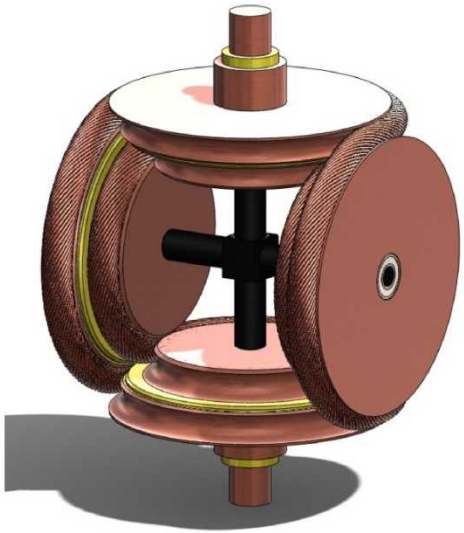

3-channel 3-phase

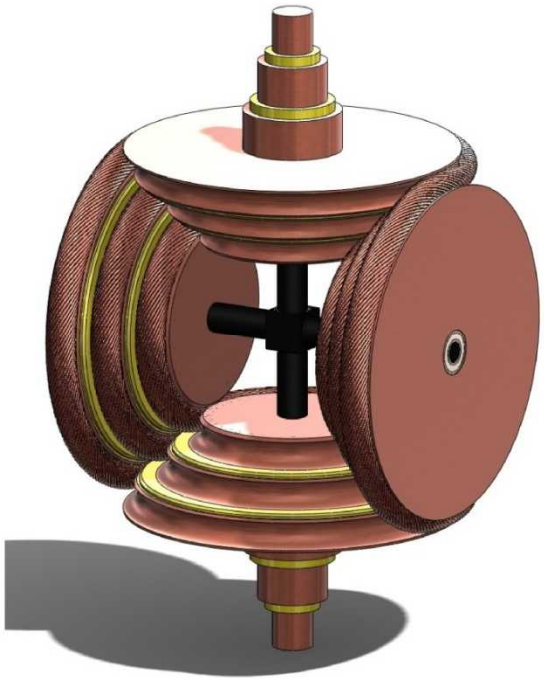

State of the art in current density

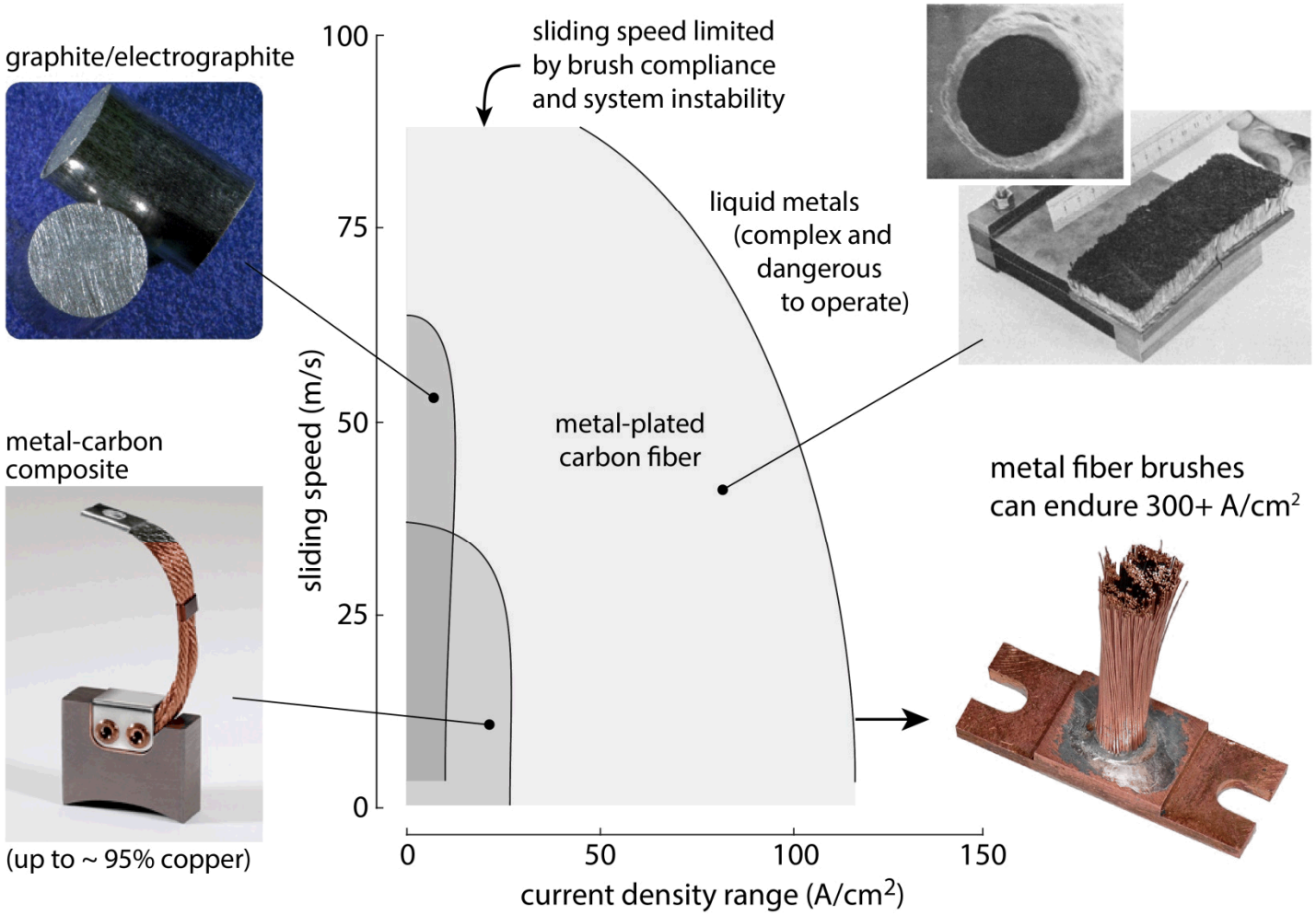

ref: Kendall, McNab, and Wilkin, Physics in Technology 6 (1975)

Unlike brushes, heating is distributed and thermal energy convected, and electrical conduction almost entirely transverse, so current densities of 1000+ A/cm^2 become practical in rolling contact

Experiment platform: "unwrapped" Twistact for accelerated aging

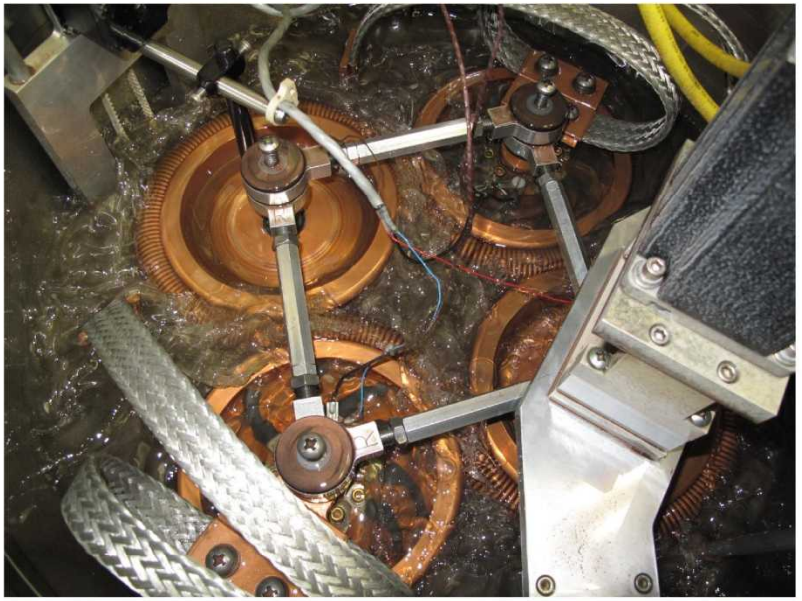

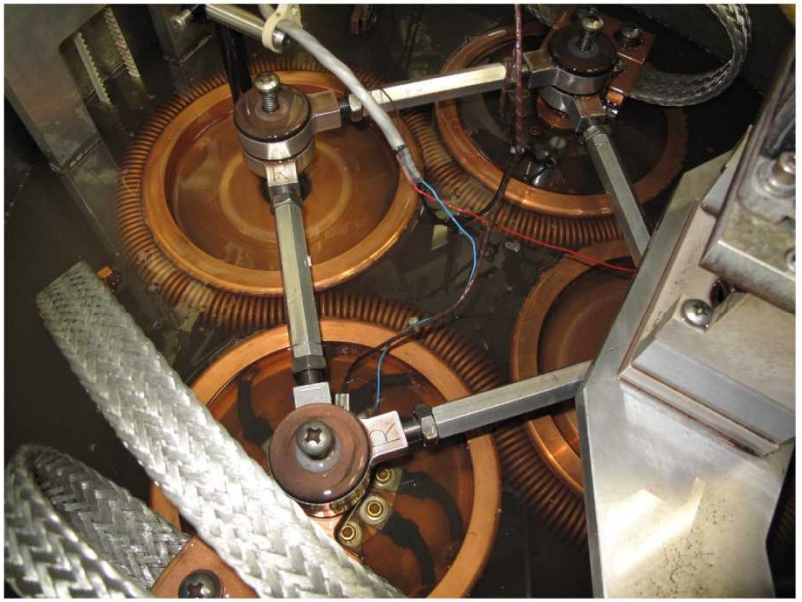

Capabilities

Up to 300 RPM operation
Up to 2kA DC continuous
Apply and measure belt tension
Closed circuit cross-flow heat exchanged (2kW)
Controlled gas and liquid immersion

Twistact Circuit Analysis

For a 25 mm diameter belt of 2.5 sq. mm. Cu wire:

$$R_{\substack{half\\winding}} = \rho_{Cu}\frac{L}{A} \cong \rho_{Cu}\frac{r_{belt}}{r_{wire}^2} \cong 107\,\mu\Omega$$

$$R_{Holm} = \frac{\rho_{Cu}}{2a} \cong \frac{\rho_{Cu}}{2}\sqrt{\frac{\pi H}{F_n}}$$

Then,

H ~ 1 GPa and

F_n ~ 45 N or 10 lbs (belt tension = half F_n):

$$R_{Holm} \cong 71\,\mu\Omega$$

where F_n is contact force and H is the hardness of the softer sheave (work hardened, OFHC).

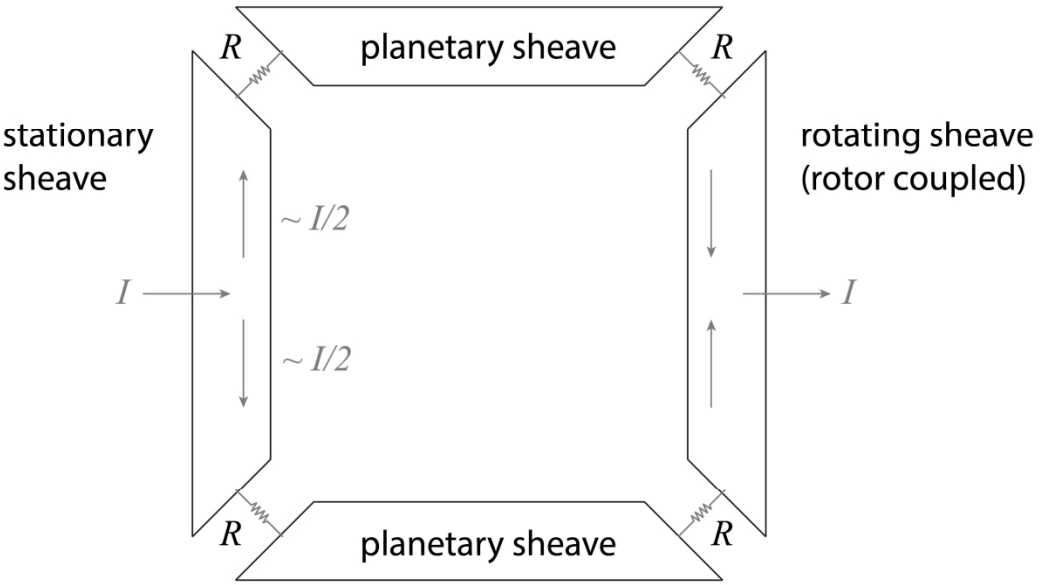

$$R_{Twistact} = \left(\frac{1}{2R} + \frac{1}{2R}\right)^{-1} = R$$

$$R = R_{\substack{one\\winding}} + 2R_{Holm}$$

(assuming negligible bulk sheave resistance)

This corresponds to a system resistance of approximately

$$R_{Twistact} \cong 0.25\,m\Omega$$

Current spends little time on belt

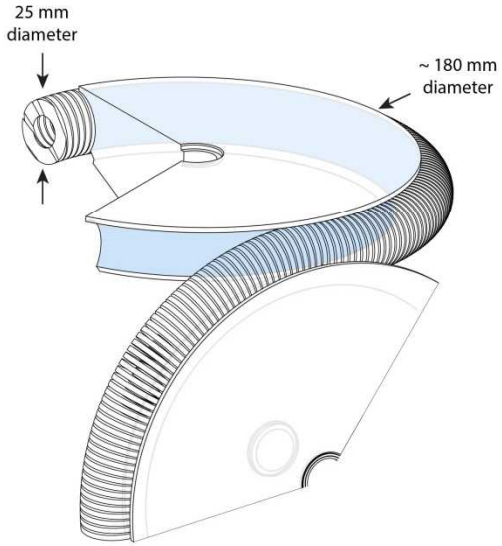

steady-state at 300A, no cooling, air exposed

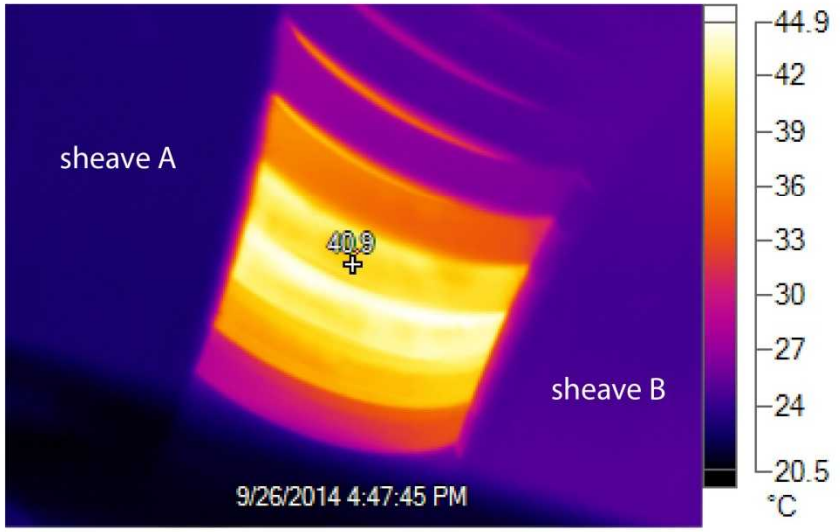

the belt/sheave contact was modeled as a network of resistors for which one contact point with the sheave occurs per winding:

(1 asperity per winding, 70 windings per sheave)

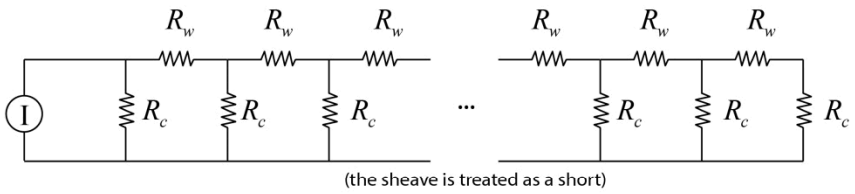

R_w is the resistance of a single length of winding $\longrightarrow$ $R_w = \rho \frac{L}{A}$ ~ 0.107 mΩ

R_c is the contact resistance at one asperity (1 per winding) $\longrightarrow$ $R_c = \frac{\rho}{2a}$ ~ 0.071 mΩ

calculated for a 10 lb belt tension

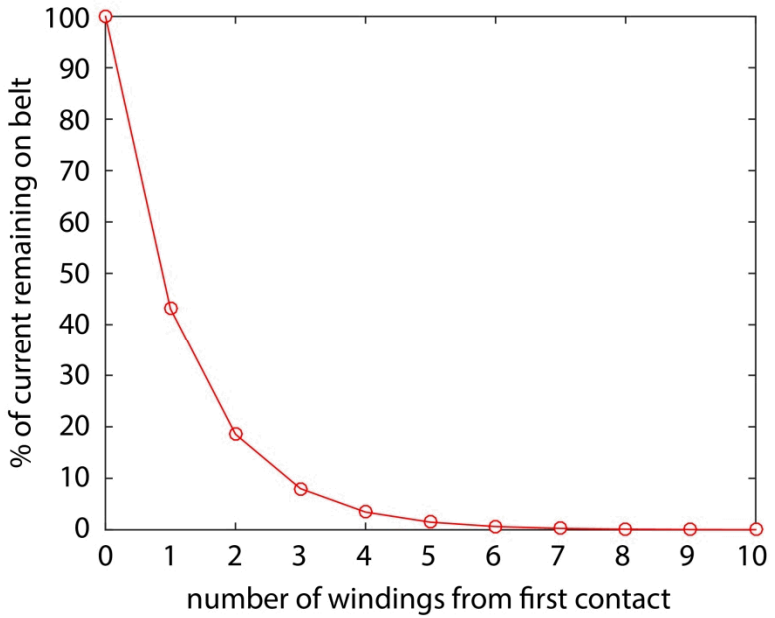

Work hardening over about 100k to 1M cycles toward steady-state resistance

Operating a belt at 10 lb tension
immersed in water with N2 cover gas
at 100 RPM

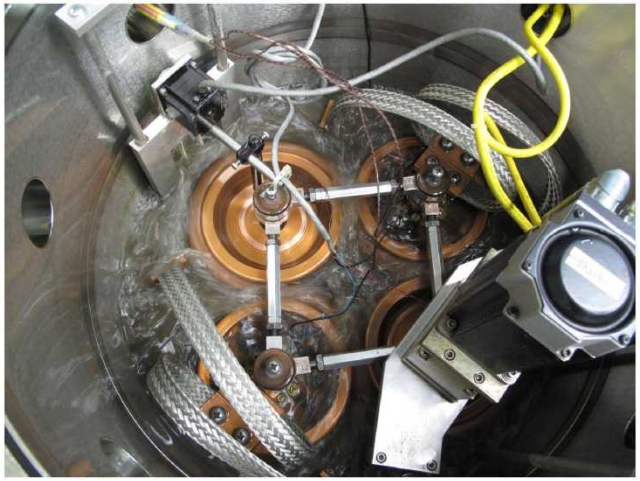

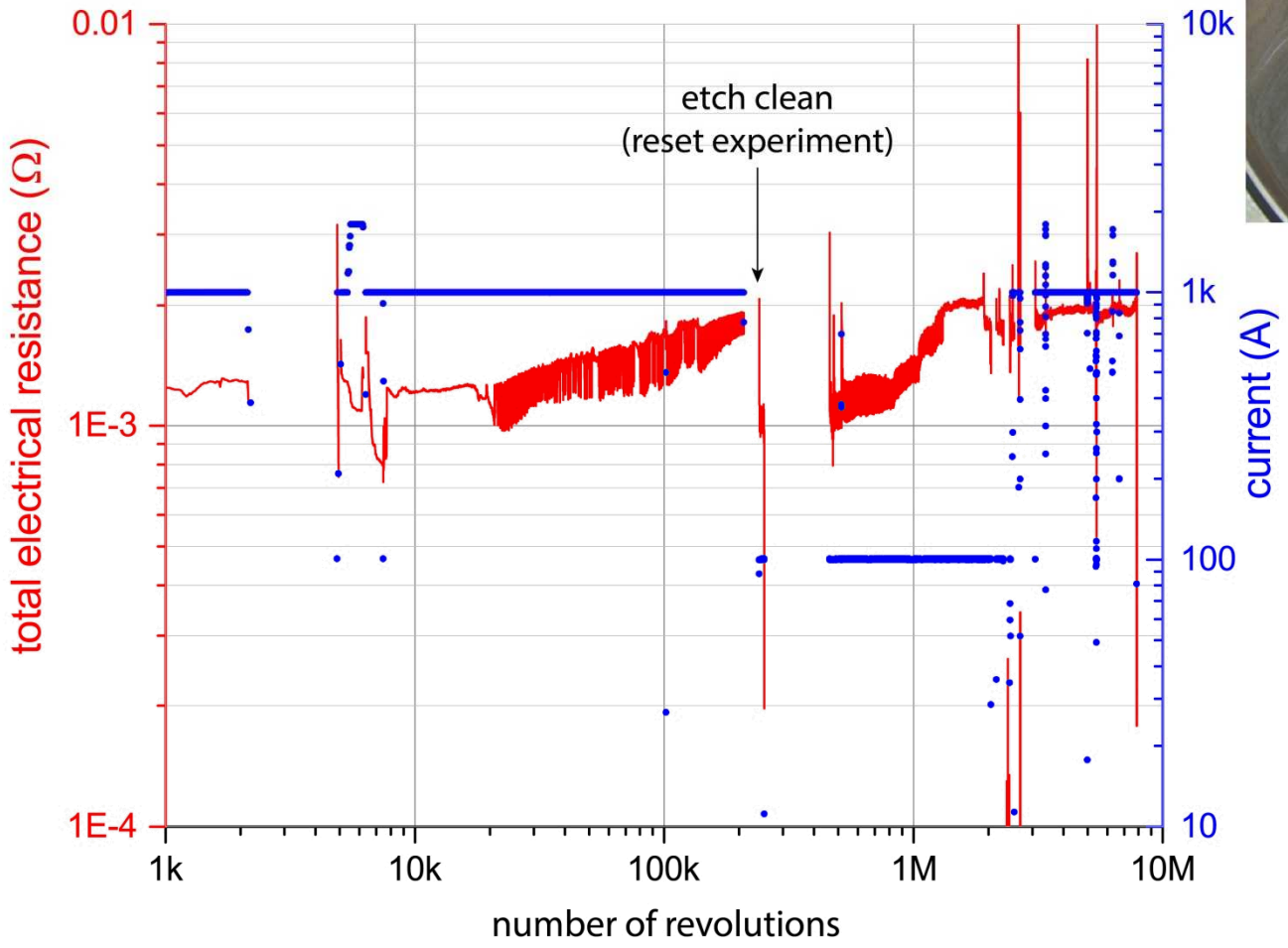

Evidence of work hardening:
2x change in resistance is
commensurate with H change

Cross-section of sheave groove after 8M cycles : polished and chemically etched

sectioned sheave

Worn-in OFHC CU sheave was sectioned, potted, polished, and acid etched to enhance grain contrast

18 mm

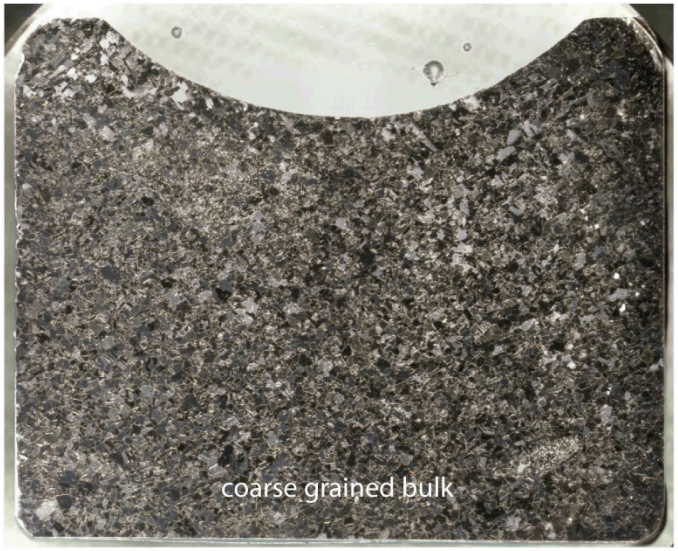

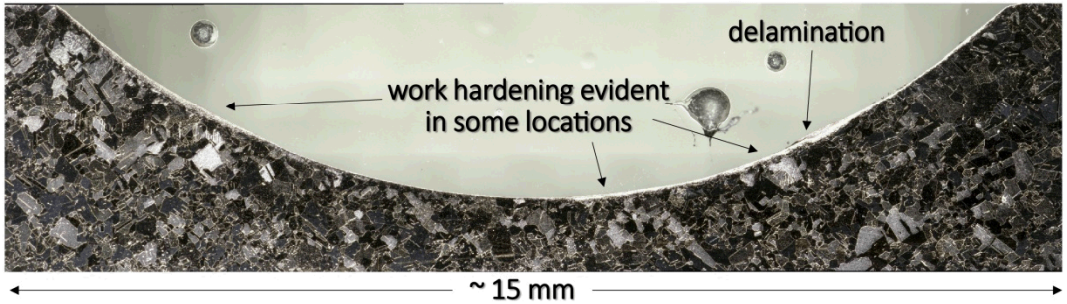

~ 15 mm

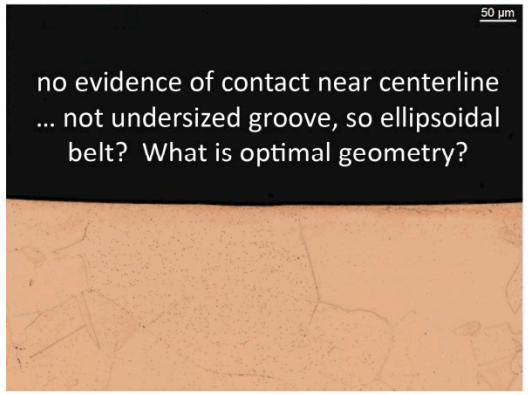

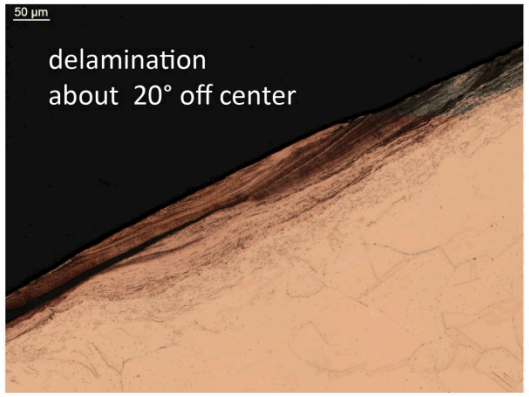

Materials Challenges at the Interface

Component Design
example: inertial switch

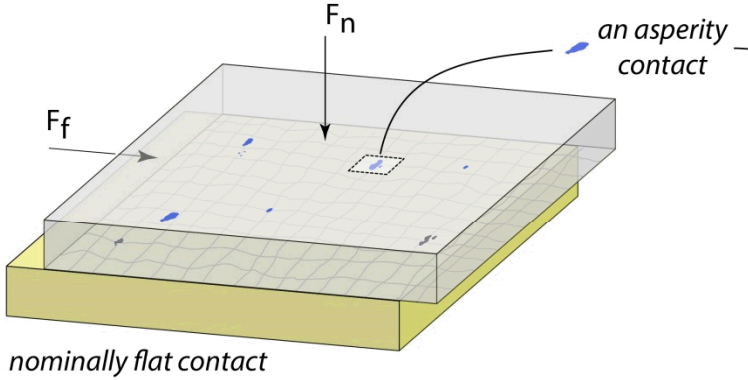

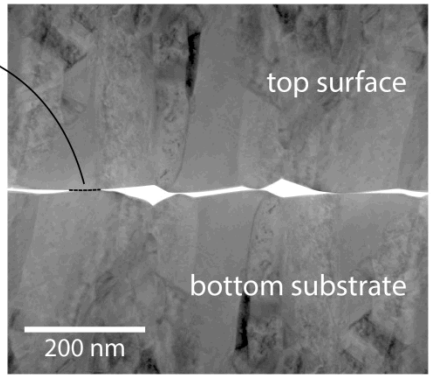

Surface Roughness
for metal contacts the real area of contact is **typically < 1% (even ppm)** *of the apparent area (Greenwood & Williamson, 1966)*

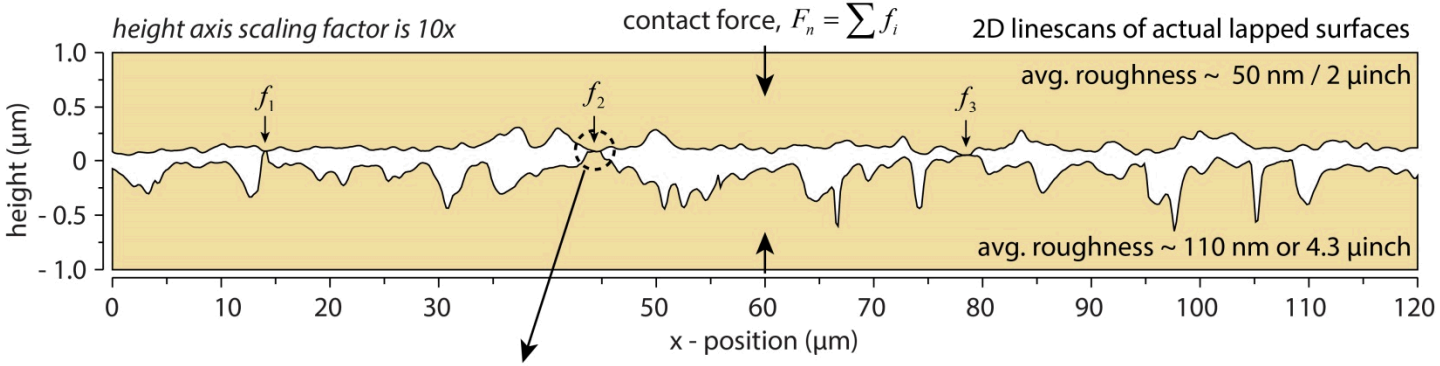

Asperity Contacts, Constriction, Asperity Contacts and Surface Films
areal sum of asperity contacts and surface films define electrical contact resistance

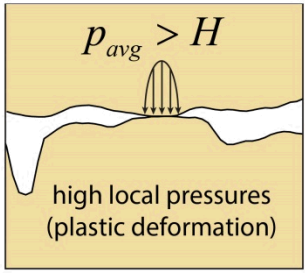

... for metal contacts the real area is a function of hardness and contact force (Bowden & Tabor, 1939):

$$A_r \cong \frac{F_n}{H}$$

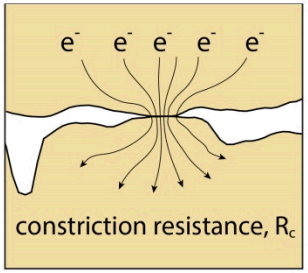

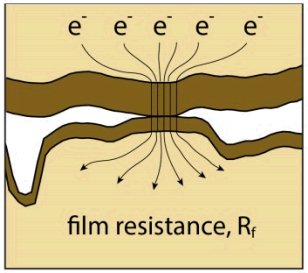

... ECR is a function of the constriction and film resistances:

$$ECR = \sum_i \left(R_{c,i} + R_{f,i} \right)$$

Two key design parameters: *wear rate* and *electrical contact resistance*

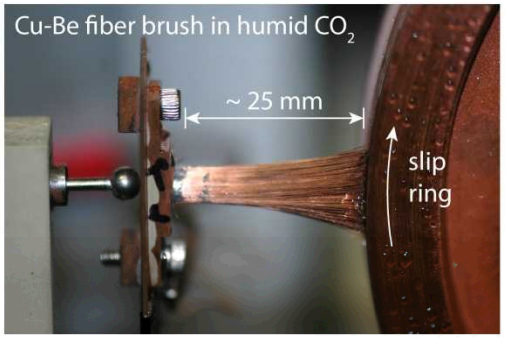

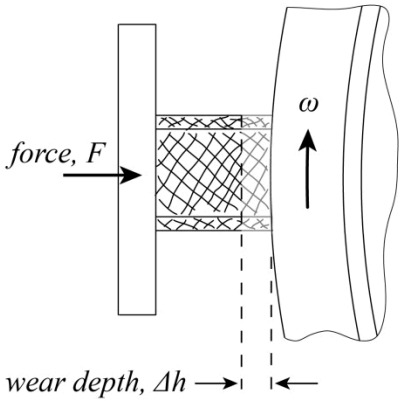

linear wear rate:

$$K_{lin} = \frac{\Delta h}{d} = \frac{wear\ depth}{sliding\ distance}$$

a comparison to specific wear rate, in units of mm^3/N-m, is achieved by dividing the linear wear rate by the brush nominal contact pressure:

$$K_s = \frac{1}{p_o} K_{lin} \left(\frac{mm^3}{N-m} \right)$$

ref: D. Kuhlmann-Wilsdorf and E. Shobert, *Sliding Electrical Contacts in* P.G. Slade (Ed.), *Electrical Contacts: Principles and Applications*, CRC Press, 1999

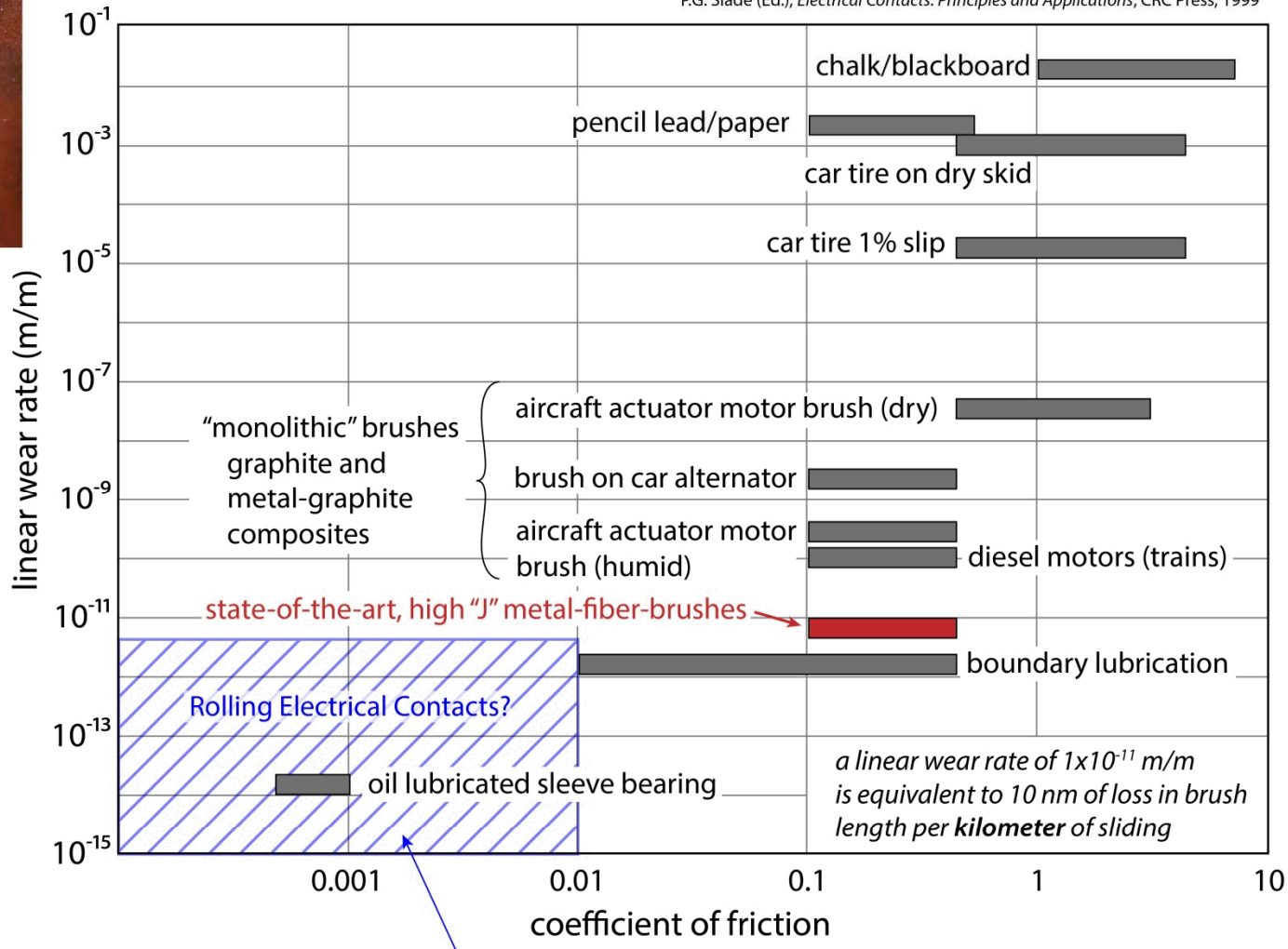

Reduced frictional losses highly beneficial for higher speed applications such as electric vehicles

Also… metal fiber brushes are susceptible to debris packing, reduced performance

Contact pressure of 15 kPa
Sliding speed of 2.5 to 7.5 m/s
Current density of 180 to 250 A/cm2
Brush fiber packing fraction ~ 0.5

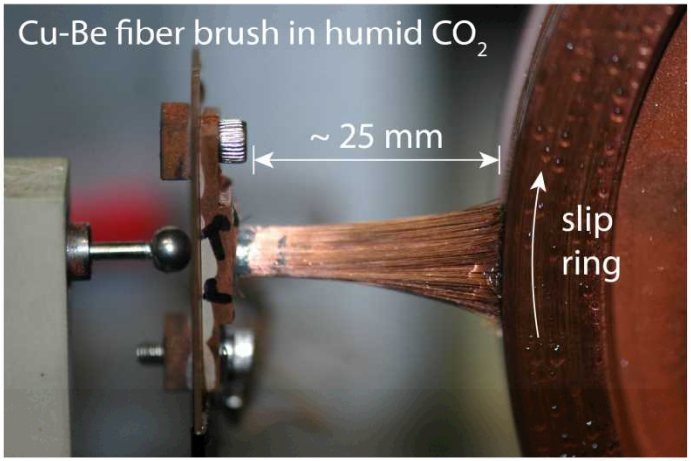

SEM micrographs of unworn brush

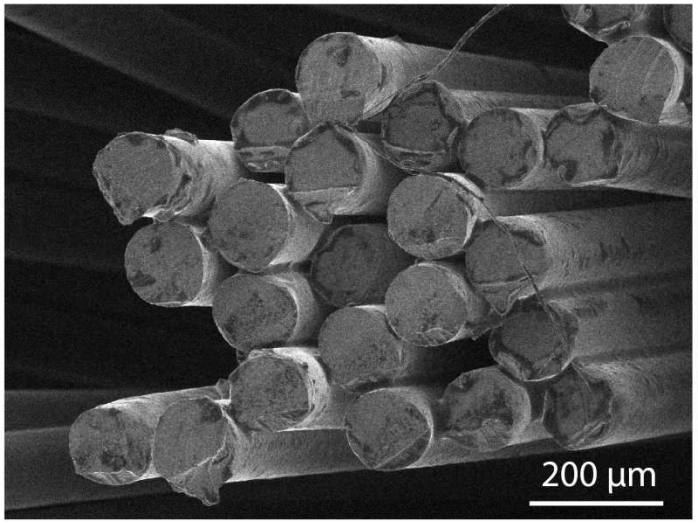

SEM micrographs of the worn fiber brush tips

After 13,000 km of sliding over 29 days; brushes lose compliance and can transition to "monolithic" brush performance:

more prone to arcing and chatter

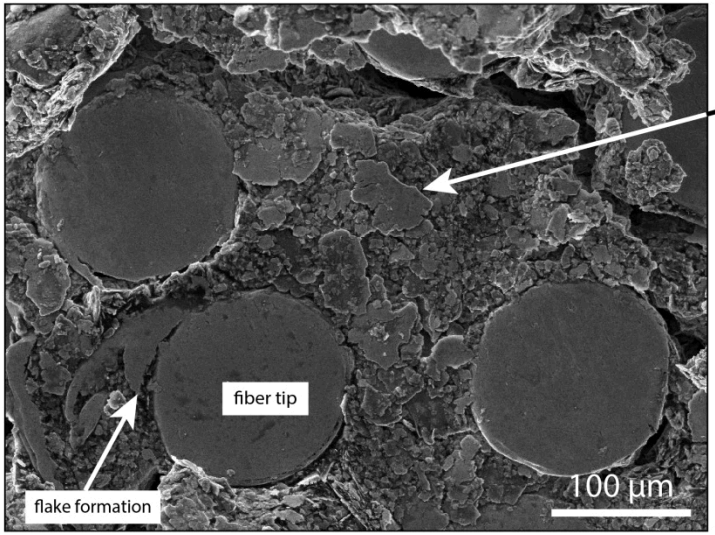

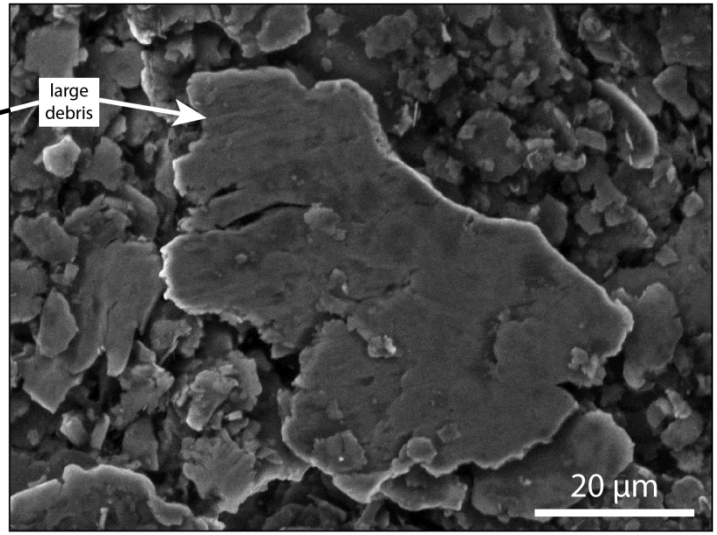

Low wear rolling electrical contacts are keenly susceptible to insulating film formation

Electrical contact resistance is strongly a function of film resistance. Lightly loaded metal rolling contacts will gradually wear primarily through surface fatigue and delamination, so the **propensity for insulating film formation is critical**

asperity contact

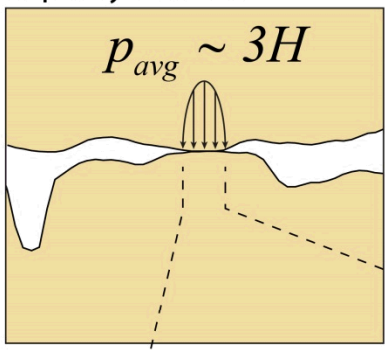

$$ECR = \sum_i \left(R_{c,i} + R_{f,i} \right)$$

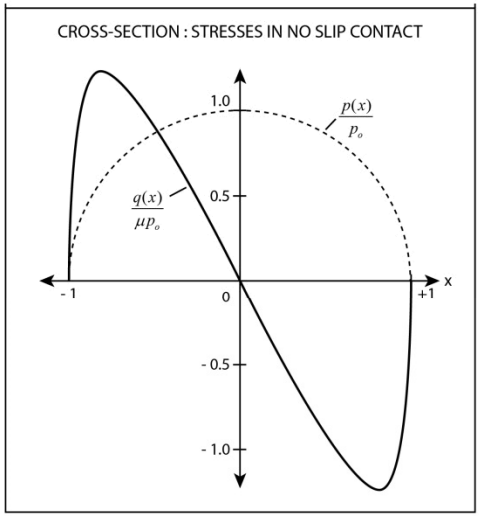

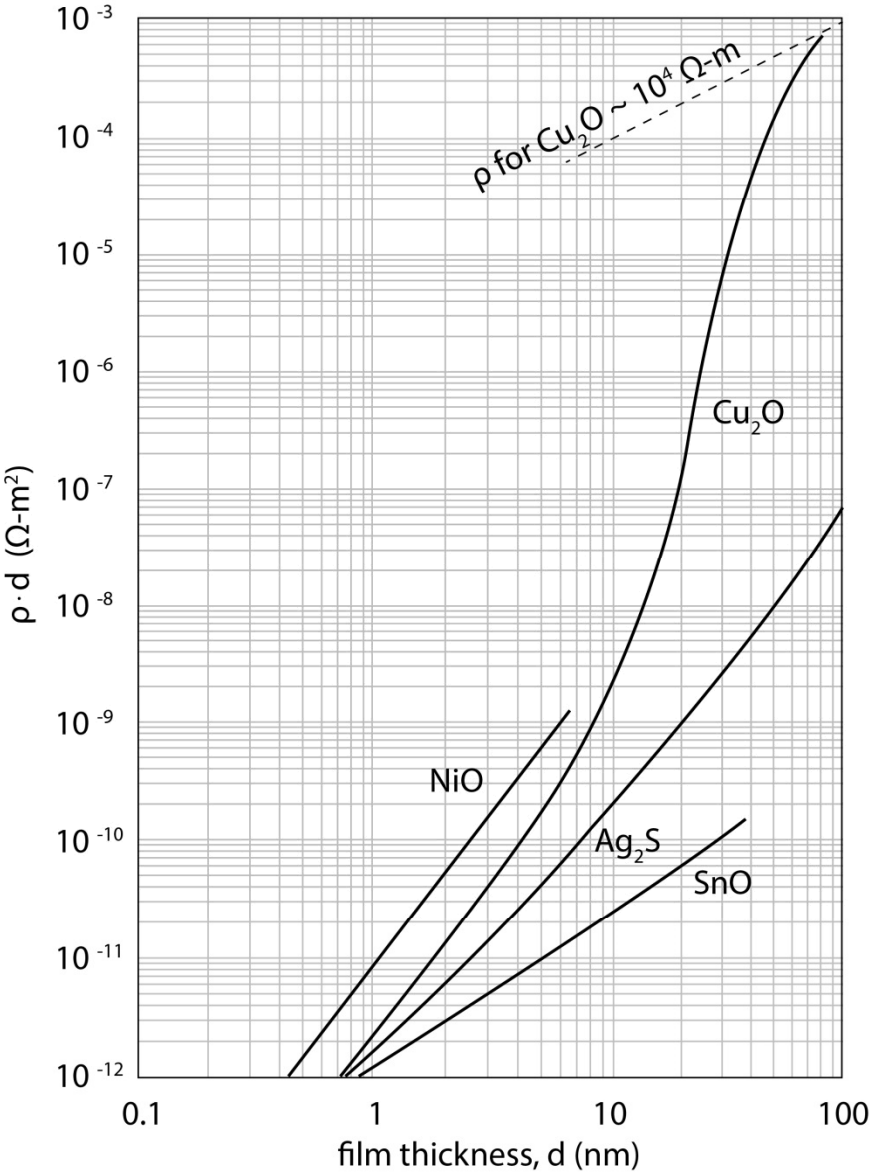

ref: R. S. Timsit, Electrical Contact Resistance in Electrical Contacts Principles and Applications, 1999

Experiments to optimize lubrication and cooling - liquid and cover gas control

Rolling electrical contact experiments with liquid lubricants/coolants to determine propensity for insulating film formation

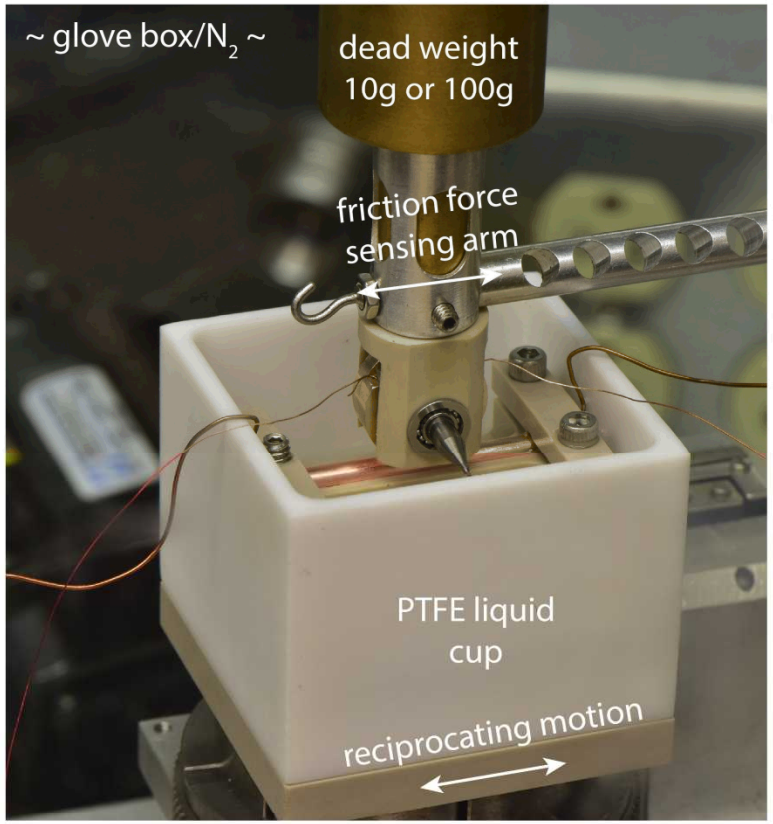

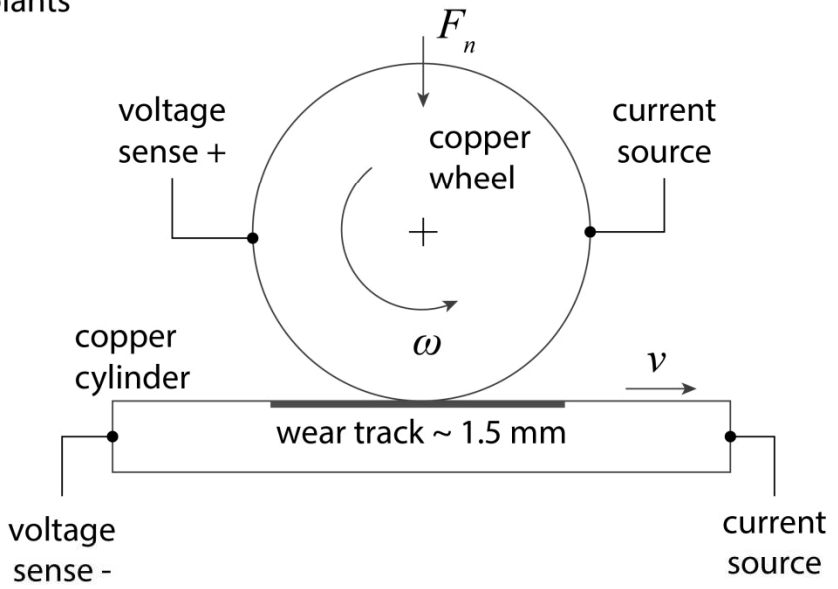

Typical experiment parameters

normal force : 1 N
max sliding speed : 5 mm/s
reciprocating frequency : 1.6 Hz
stoke length : 1.5 mm
probe current: 100 mA

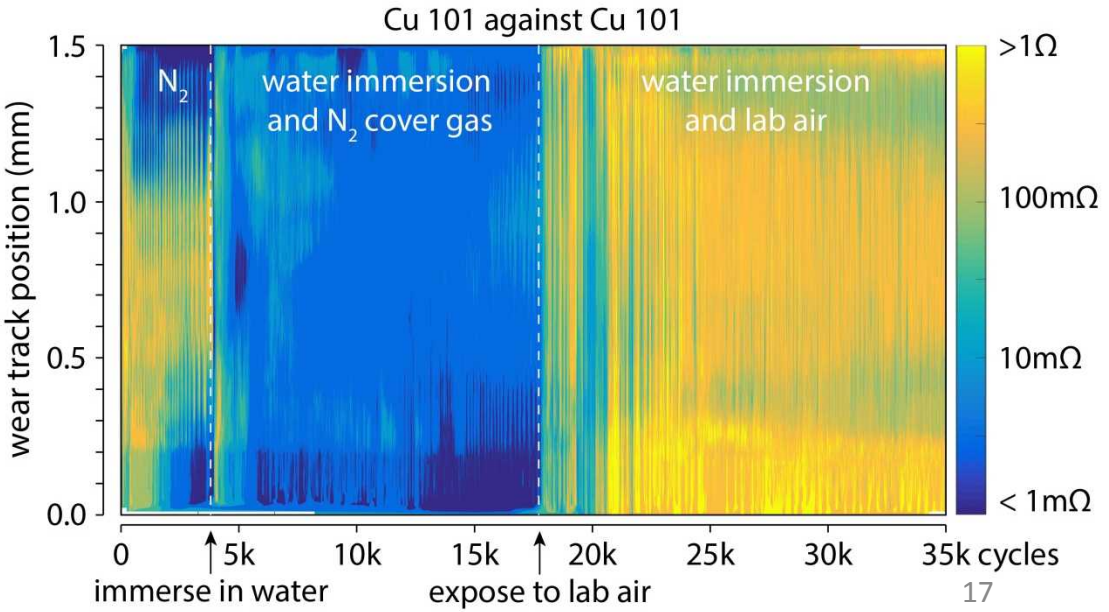

Ongoing experiments with high dielectric strength liquid lubricants/coolants

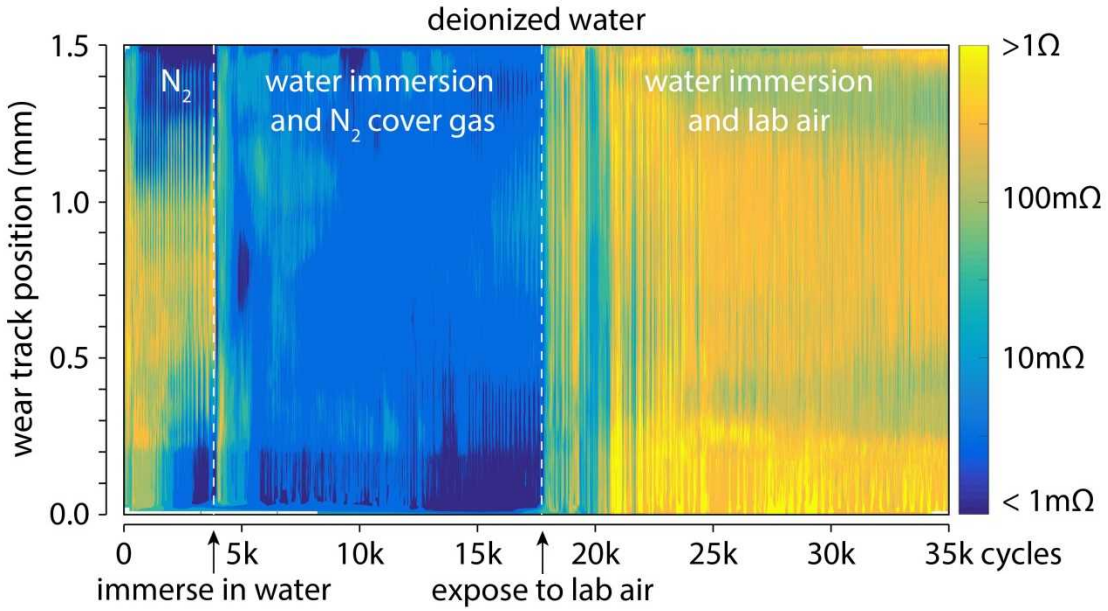

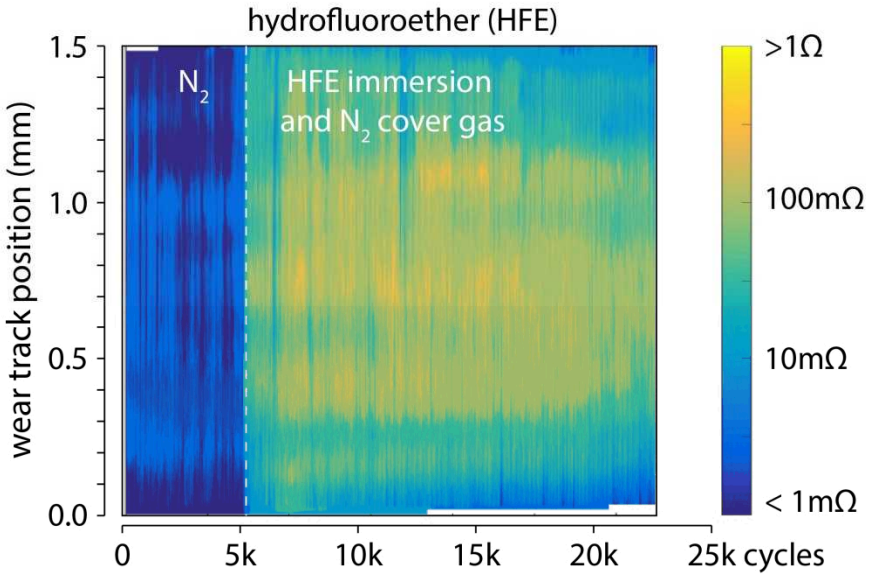

Ongoing experiments with high dielectric strength liquid lubricants/coolants

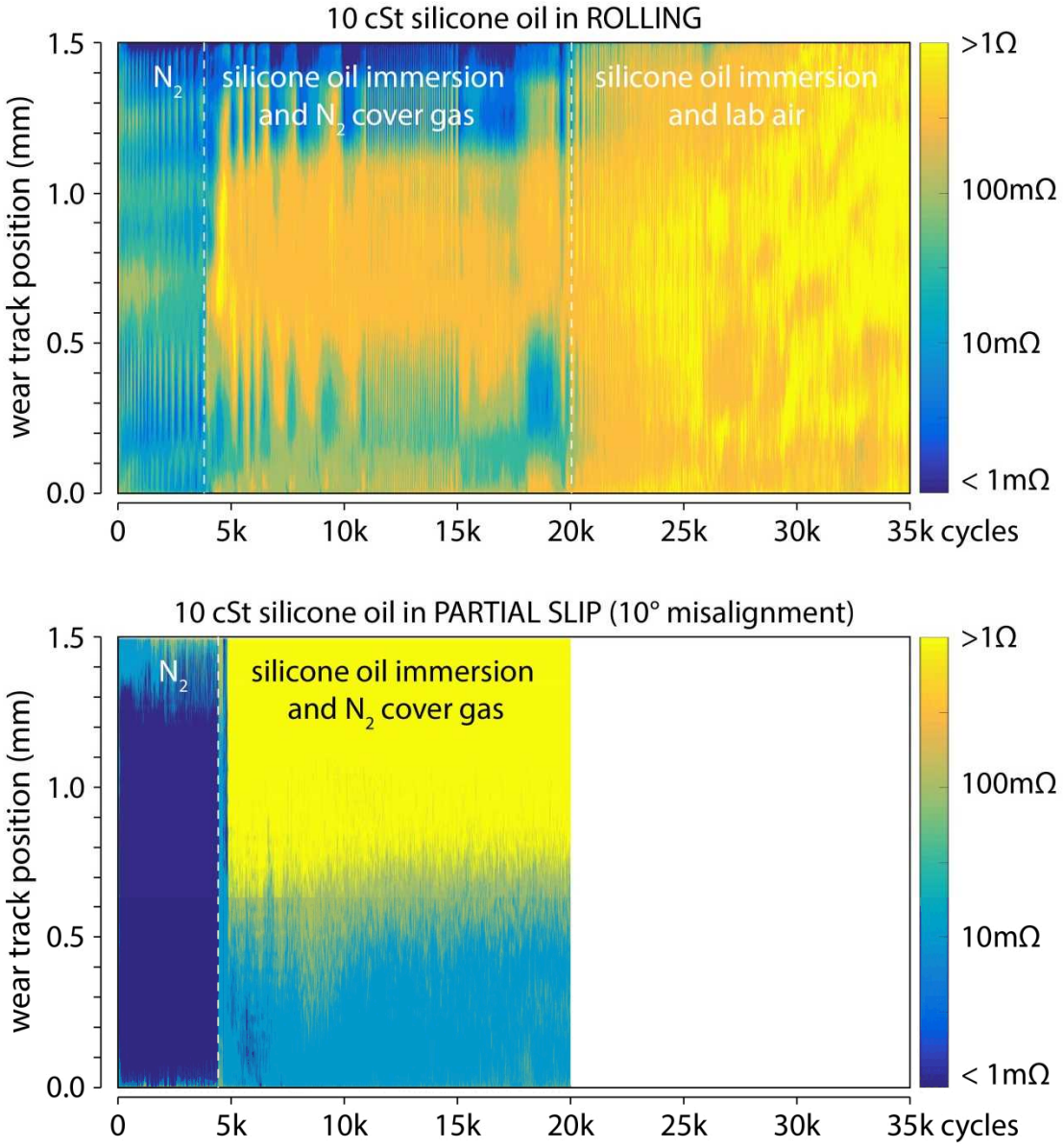

Sliding induced formation of a thick insulating film!

Questions?

Appendix Slides

For off-shore wind harvesting, most generator topologies are off the table...

Table 1: Pros and cons of different generator architectures in the context of multi-MW wind turbines

drive train	generator type	rotor architecture	advantages	disadvantages
gearbox	induction	squirrel cage	no rare earth magnets no brush/slip-ring maintenance	gear box failures *DFIG counterpart cheaper*
gearbox	induction	wire-wound	no rare earth magnets	gear box failures brush/slip-ring maintenance
gearbox	synchronous	wire-wound	no rare earth magnets	gear box failures brush/slip-ring maintenance *DFIG counterpart cheaper*
gearbox	synchronous	permanent magnet	no brush/slip-ring maintenance	gear box failures rare earth magnets (25 kg Nd /MW)
direct-drive	induction	squirrel cage	no gear box failures no rare earth magnets no brush/slip-ring maintenance	*poor power factor*
direct-drive	induction	wire-wound	no gear box failures no rare-earth magnets	*poor power factor* brush/slip-ring maintenance
direct-drive	synchronous	wire-wound	no gear box failures no rare earth magnets	brush/slip-ring maintenance
direct-drive	synchronous	permanent magnet	no gear box failures no brush/slip-ring maintenance	rare-earth magnets (250 kg Nd /MW)
direct-drive	synchronous	wire-wound+Twistact	no gear box failures no rare earth magnets no brush/slip-ring maintenance	

DFIG: doubly-fed induction generator; Nd: Neodymium

Delamination wear… a trip back in time: 1926 and the "Roscoe Effect"

In 1926, R. Roscoe reported postulated that metals covered by hard, thin surface films or oxides exhibit increased hardness of the metal in the vicinity of the surface, leading to **embrittlement of otherwise ductile materials**

(microscopy observation of dislocations was not yet available)

Evidence of Roscoe Effect on Au single crystals

Wear track on gold single crystal with a $AuCl_3$ layer, sliding in the [110] direction.

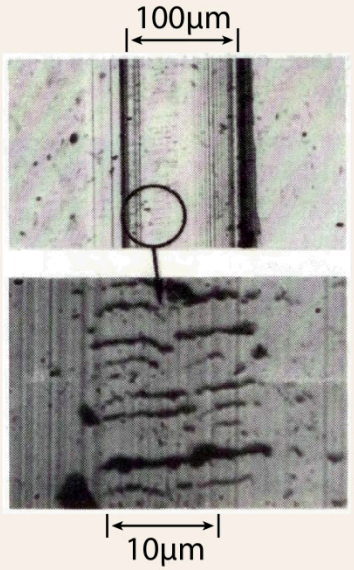

surface of Au wear track, no cracking

surface of $AuCl_3$ wear track, surface cracks

D.H. Buckley, Surface Effects in Adhesion, Friction, Wear, and Lubrication, Tribology series 5, Elsevier 1981

On to the *"Swinging Sixties"*... and the work of Shen, Wood, and Duquette et al.

Wood, Cousland and Sargant suggested that the increased void formation rate in the presence of surface oxides described leads to an increase in crack propagation rates.

- Wood et al, Acta Metallurgica, 11 (1963)

Shen, Podlaseck and Kramer proposed mechanism for accelerated crack nucleation and growth (based on experimental evidence on aluminum):

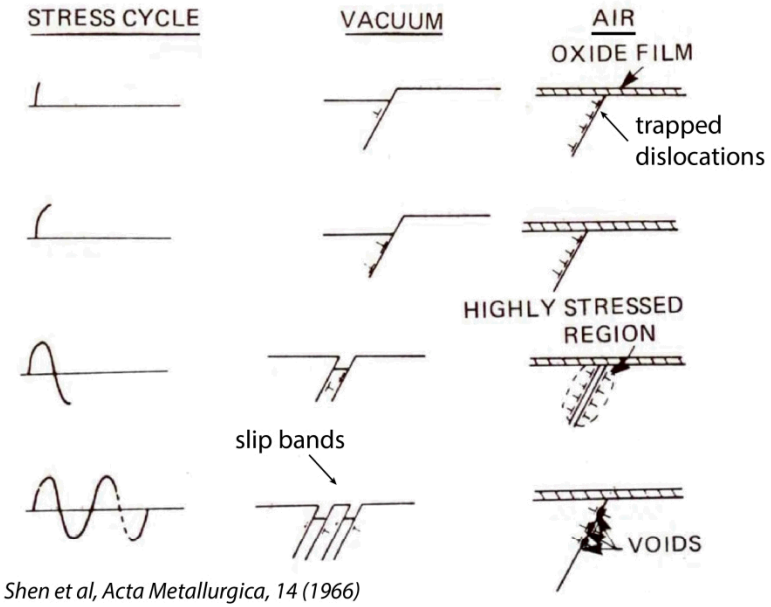

Shen et al, Acta Metallurgica, 14 (1966)

Further demonstrated by Duquette and Gell during investigations of fatigue life of Ni-based superalloy foils

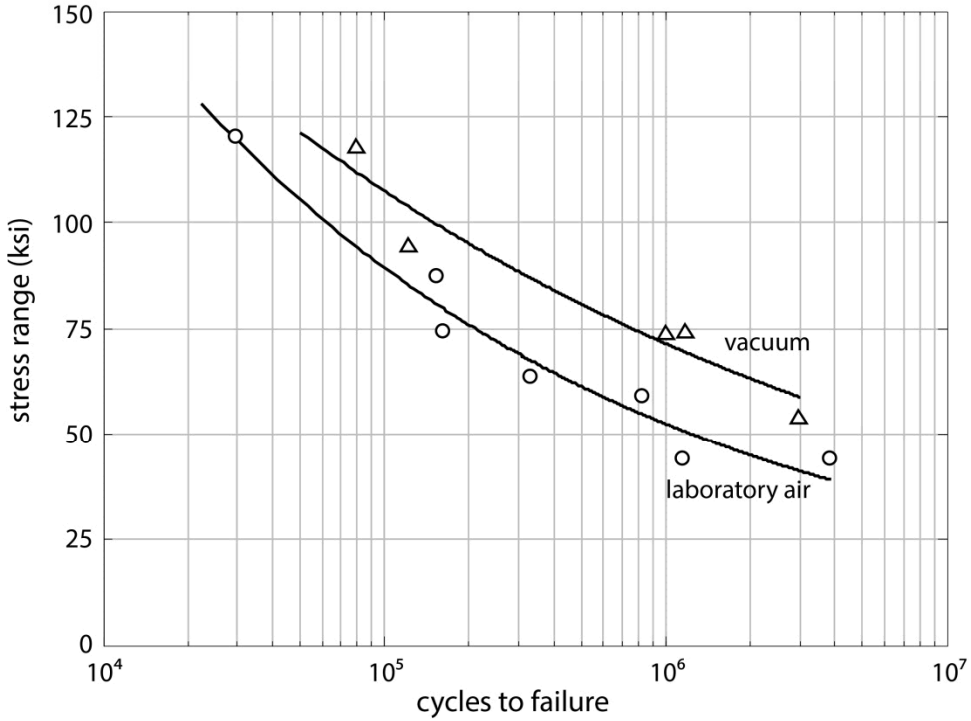

D.J. Duquette and M. Gell, Metallurgical and Materials Transactions, vol. 2, no. 5 (1971)

For low wear metal contacts, delamination is the principal wear mechanism. Fatigue strength drives wear rates, and the removal of surface insulating films and oxides.

More recent work further demonstrates dislocation trapping by hard surface films

Experiments: cross-sectional TEM

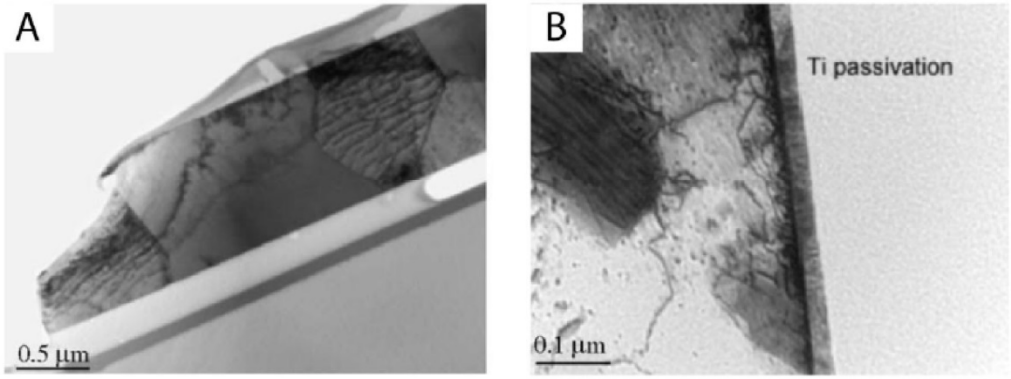

ref: Nicola, et al. Mechanics and Physics of Solids vol. 54, issue 10 (2006)

Modeling: 8-grain long films in cross-section

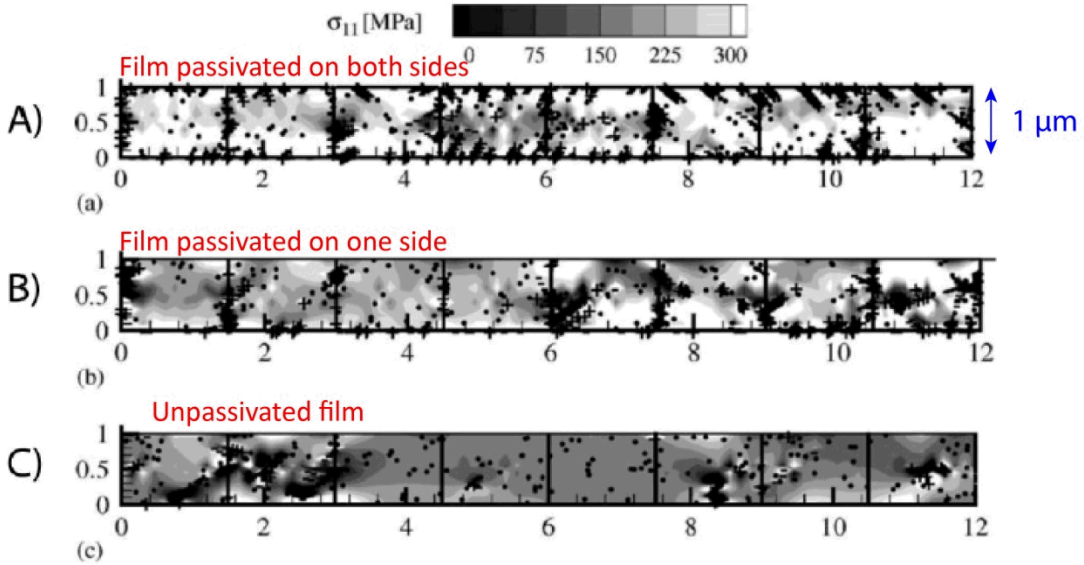

ref: Nicola, et al. Mechanics and Physics of Solids vol. 54, issue 10 (2006)

Passivation leads to enhanced film strain (4x higher)

Ultra-low wear of metal contacts primarily occurs via *delamination*

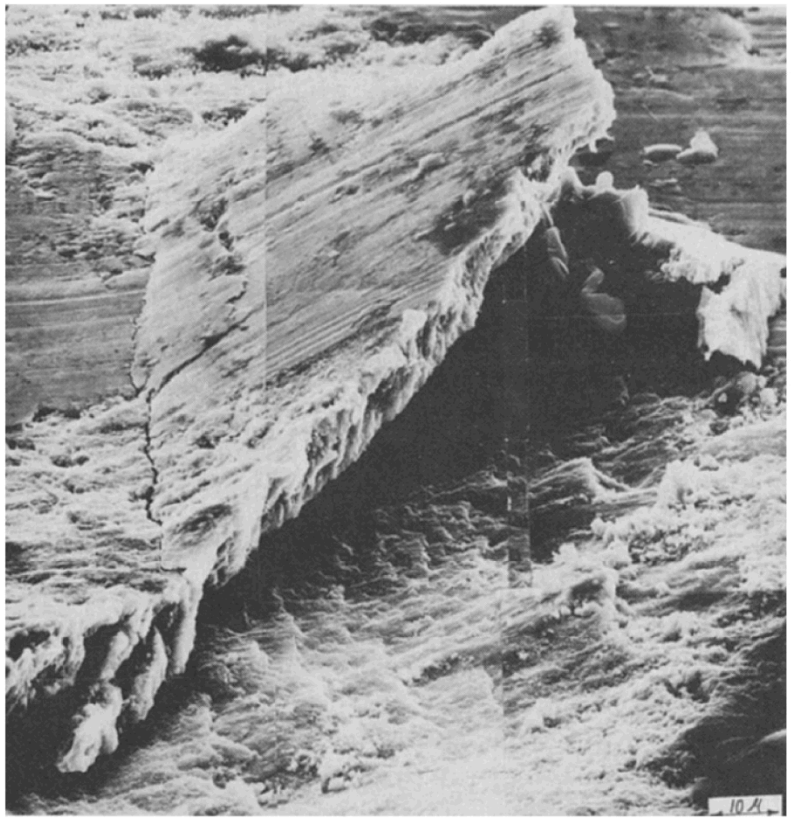

Fig. 4. Wear sheet formation in an iron solid solution. Note that the sheet is lifting up opposite to the sliding direction. (The sliding direction is from right to left.)

Nam P. Suh "An overview of the Delamination Theory of Wear" Wear, 44 (1977) pp. 1-16

Collected wear debris from samples that were run in wet carbon dioxide is thin and flake-like. X-ray diffraction studies reveal that it is predominantly copper as opposed to cuprite, which is seen in open air experiments.

- Irwin Singer (2006)

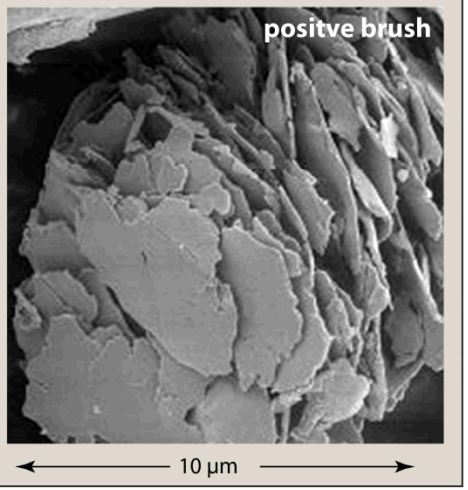

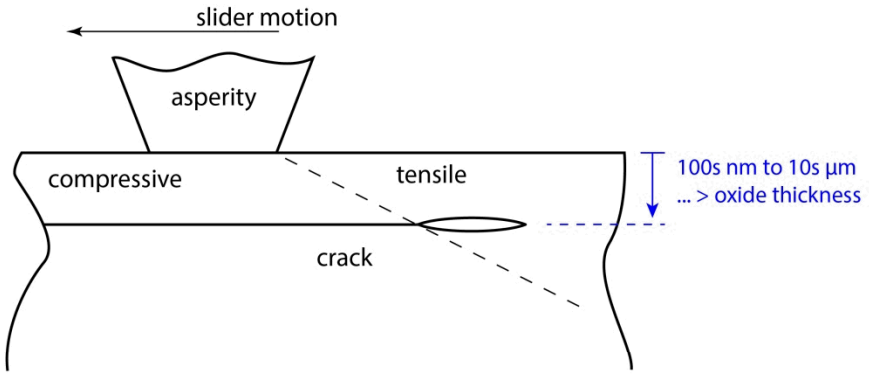

Fig. 1. A model of a subsurface crack in sliding contact

J. R. Fleming and Nam P. Suh "Mechanics of Crack Propagation in Delamination Wear" Wear, 44 (1977) pp. 39-56

Delamination events tend to nucleate well below the oxide or surface films, producing lamellar particles on the order of 1 to 10 μm thick.

At sufficiently high contact voltage: enhanced oxidation/reduction!

Modified Mott-Cabrera Model

proposed by Boyer, Noel, Chabrerie in Wear 116 (1987), pp 43-57

In a well known model for oxidation of metals, Cabrera and Mott postulated that the electrons can pass freely from the metal to the surface of the oxide through a uniform field within the oxide. Once the electrons arrive at the oxide surface they are free to ionize the oxygen atoms.

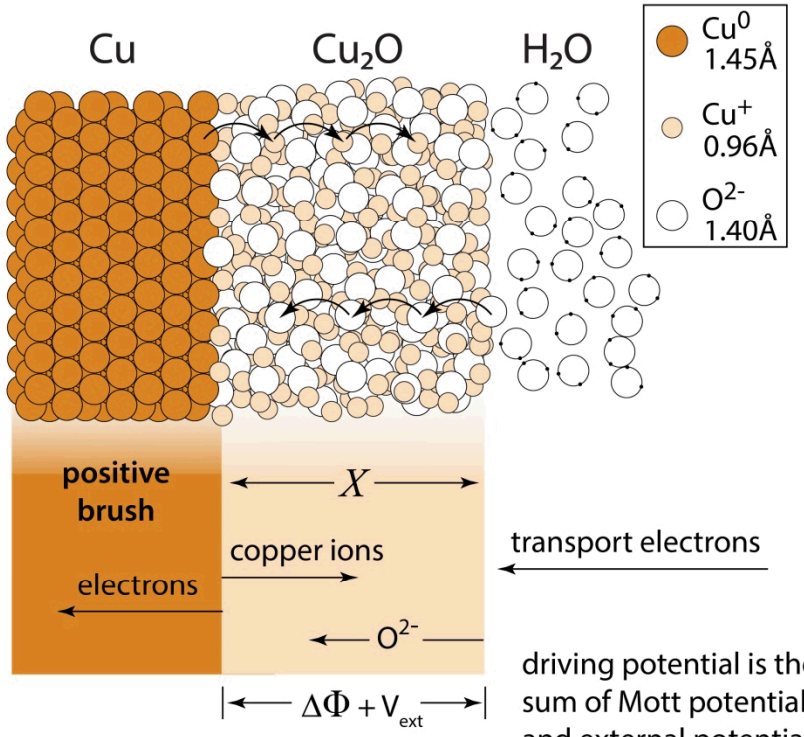

activation energy for a metal atom to ionize and jump into the oxide

an externally supplied potential

$$\frac{dX}{dt} = av\exp\left(\frac{-W}{kT}\right)\exp\left(\frac{qa\Delta\Phi}{2kTX}\right)\exp\left(\frac{qa\Delta V_{ext}}{2kTX}\right)$$

rate of oxide formation

in the absence of an externally supplied potential this is the ratio of the limiting film thickness and the current film thickness

$$\frac{\dot{X}_{+\,brush}}{\dot{X}_{-\,brush}} = \exp\left[\frac{qa\left(V_{+} - V_{-}\right)}{2kTX}\right]$$

Cabrera and Mott's theory predicted the effects of increased oxidation rates under positive externally applied fields. The Mott potential for copper is ~ **700 mV**. The voltages across a sliding electrical contact at high current density are of the same order.

$$\frac{\dot{X}_{+\,brush}}{\dot{X}_{-\,brush}} \cong 2 \text{ to } 20x$$

Why does humidified CO2 produce low wear and contact resistance?

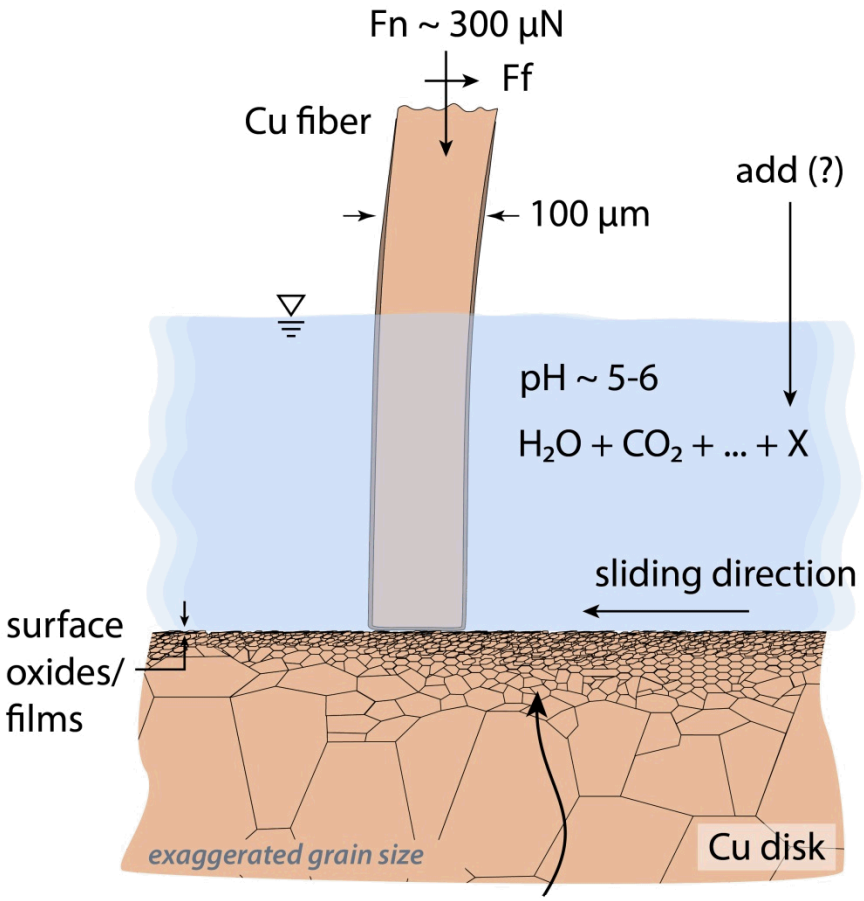

Pourbaix diagram for Cu-CO_2-H_2O System at 25°C

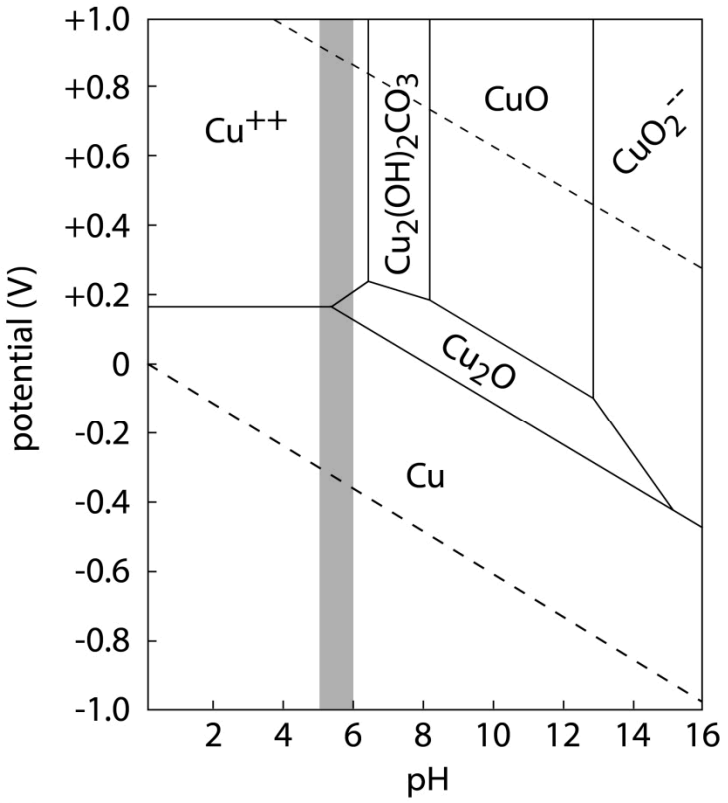

Taylor and Cannington, (1993).

What are the roles of surface films, subsurface deformation, and electrical current transport on the friction, wear, and contact resistance of metal sliding electrical contacts?